Journal of Physics: Conference Series

PAPER • **OPEN ACCESS**

The Interaction of Current Sheets with a Shock Wave and Particle Acceleration

To cite this article: Masaru Nakanotani *et al* 2020 *J. Phys.: Conf. Ser.* **1620** 012014

View the article online for updates and enhancements.

IOP ebooks™

Bringing together innovative digital publishing with leading authors from the global scientific community.

Start exploring the collection–download the first chapter of every title for free.

This content was downloaded from IP address 108.81.184.87 on 04/10/2020 at 17:57

Journal of Physics: Conference Series **1620** (2020) 012014 doi:10.1088/1742-6596/1620/1/012014

The Interaction of Current Sheets with a Shock Wave and Particle Acceleration

Masaru Nakanotani[1], Gary P. Zank[1,2] and Lingling Zhao[1]

[1] Center for Space Plasma and Aeronomic Research (CSPAR), University of Alabama in Huntsville, Huntsville, AL 35899, USA

[2] Department of Space Science, University of Alabama in Huntsville, Huntsville, AL 35899, USA

E-mail: mn0052@uah.edu

Abstract. We investigate the interaction of a shock wave with multiple current sheets using a 2D hybrid simulation. We set the separation between current sheets at $25c/\omega_i$ and the thickness longer than the ion inertial length. While the current sheets are stable upstream, they become unstable to the tearing instability since the thickness becomes shorter than the ion inertial length after they interact with the shock wave. Magnetic islands produced by the instability evolve into larger islands through coalescence and the electromagnetic fields become turbulent far downstream. We also observe that the number of energetic particles increases with distance away from the shock wave and that the increase corresponds to the evolution of the current sheets.

1. Introduction

Several studies show that particle flux is enhanced continuously downstream of heliospheric shock waves. Voyager 1 and 2 observed that the anomalous cosmic ray (ACR) intensity continued to increase after crossing the termination shock (TS) [1, 2]. The same behavior was observed at an interplanetary shock in the heliosphere observed by the Ulyssess spacecraft near 5 au [3]. These flux enhancements cannot be explained by the classical diffusive shock acceleration mechanism, which is considered to be the standard model for particle acceleration by a shock wave, because the flux intensity should peak at the shock wave and not downstream according to the theory.

Zank et al. [4] developed a model that allows for the possibility of energetic particle flux enhancements behind the shock as a result of downstream magnetic reconnection processes allied with DSA. The particle energization is due to turbulent magnetic reconnection associated with the anti-reconnection electric field, magnetic island merging, and magnetic island contraction. Although magnetic reconnection downstream of a shock wave can be thought of as primarily a mechanism to energize charged particles, it is not clear how current sheets (CSs) that might be responsible for magnetic reconnection are produced downstream. Here, we consider the possibility that heliospheric current sheets are a source of magnetic reconnection downstream of a shock wave.

Particle energization in multiple CSs has been investigated using kinetic simulations. Drake et al. [5] performed a 2D full particle-in-cell (PIC) simulation of multiple current sheets using doubly periodic boundary conditions. They found that protons and electrons are effectively accelerated during magnetic island merging. Burgess et al. [6] studied the evolution of multiple


Content from this work may be used under the terms of the Creative Commons Attribution 3.0 licence. Any further distribution of this work must maintain attribution to the author(s) and the title of the work, journal citation and DOI.
Published under licence by IOP Publishing Ltd

current sheets in a 3D hybrid simulation. At the final state of their simulation, the spectrum of magnetic field fluctuations exhibited a power law. In their simulation, efficient particle energization was not observed.

Although a few kinetic simulations have been performed to investigate the interaction of current sheets with a shock wave [7, 8, 9], none of them is designed for magnetic reconnection at current sheets. For example, Giacalone & Burgess [9] performed a 2D hybrid simulation of the interaction between a shock wave and current sheets inclined relative to the shock normal. They showed that pickup ions (PUIs) can escape upstream from the shock wave by moving along the current sheet. Since the mean magnetic field in their simulation is out of plane, magnetic reconnection at those current sheets does not occur.

In an astrophysical context, Sironi & Spitkovsky [10] carried out a simulation of the interaction of a relativistic shock wave with multiple current sheets whose mean magnetic field had an in-plane magnetic field. Their simulation is a full PIC simulation of an electron-positron plasma. Although they found efficient particle energization in the system, particles were mainly accelerated at reconnected current sheets upstream of the shock wave.

We present for the first time a hybrid kinetic simulation in a system similar to that of [10] to investigate the evolution of multiple CSs. In section 2, we briefly explain our numerical method, the simulation setup, and the parameters. Our results are presented and summarized in sections 3 and 4, respectively.

2. Numerical Model

We use 2D hybrid particle-in-cell (PIC) simulations to investigate the interaction of current sheets with a shock wave. Hybrid simulations treat ions and electrons as particles and a fluid, respectively. This enables us to resolve ion velocity distribution functions. We assume that the electron fluid is massless. Hybrid simulations have been extensively used to study ion scale kinetic physics [11].

The simulation domain is a 2D Cartesian geometry (x-y) and the size is $(L_x \times L_y) = (200c/\omega_i \times 204.8c/\omega_i)$ where c/ω_i is the ion inertial length. The grid size is $\Delta x = \Delta y = 0.2c/\omega_i$. The plasma is injected from the left boundary with a speed of $2V_A$ where V_A is the Alfvén speed. We set the right boundary as a conducting wall that reflects the plasma, which leads to the formation of a shock wave that propagates leftward. The simulation frame corresponds to the downstream rest frame. Periodic boundary conditions are adopted in the y direction.

The upstream plasma flow carries current sheets (CSs) following the setup of [10]. The upstream magnetic fields are described as,

$$B_x = 0; \tag{1}$$

$$B_y = B_0 \tanh\left[\frac{1}{\delta}\cos\left\{\frac{2\pi\left(x + V_{inj}t\right)}{\lambda}\right\}\right]; \tag{2}$$

$$B_z = B_0 \,\mathrm{sech}\left[\frac{1}{\delta}\cos\left\{\frac{2\pi\left(x + V_{inj}t\right)}{\lambda}\right\}\right], \tag{3}$$

where B_0 is the magnitude of the upstream magnetic field and V_{inj} is the speed of the upstream plasma flow, which corresponds to $2V_A$ in our case. Here, δ and λ determine the thickness of a CS and the separation between CSs. We set $\delta = 0.1$ and $\lambda = 50c/\omega_i$. The thickness of the CSs upstream is larger than the ion inertial length. Although the separation is much less than the real separation for heliospheric current sheets, it is still larger than the Larmor radius of the upstream plasma. This configuration satisfies the force-free condition in which the temperature and the density of plasma are constant. The CSs are perpendicular to the $x-$axis and hence parallel to the shock normal.

We use the Buneman-Boris method to push the particles and the CAM-CL method to advance electromagnetic fields. We use a time step of $\Delta t = 0.01\Omega_i^{-1}$ where Ω_i is the ion cyclotron frequency. The number of particles upstream is 100 per cell and the ion and electron plasma beta is set to $\beta_i = \beta_e = 0.5$.

3. Results

Fig. 1 shows the space-time evolution of the ion density. The shock wave propagates leftward with a speed of $\sim 1.2V_A$ corresponding to the black dashed line. The shock speed is almost constant throughout the simulation time. The resultant Alfvén Mach number in the shock rest frame corresponds to ~ 3.2, which indicates that the shock wave is supercritical. The brown stripes seen upstream in Fig. 1 correspond to CSs.

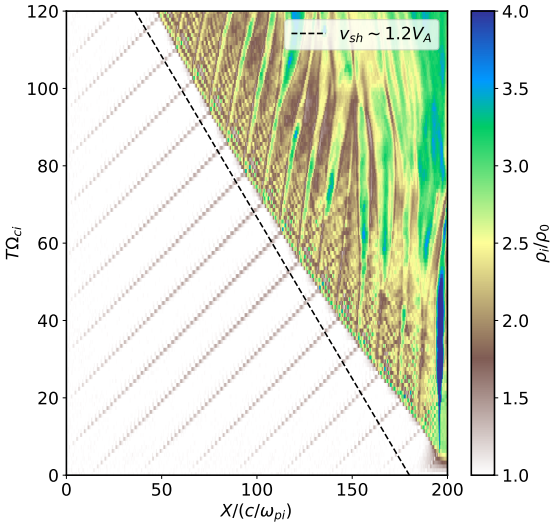

Figure 1. Space-time evolution of the ion density. The horizontal and vertical axes indicate the space and time coordinates, respectively. A shock wave forms at the right boundary and propagates leftward. The slope of black dashed line corresponds to the speed $\sim 1.2V_A$.

Fig. 2 shows snapshots of B_y, B_z, and the ion density from left to right respectively at $T = 100\Omega_i^{-1}$. The shock wave is located near $65c/\omega_i$. The separation between CSs reduces from $25c/\omega_i$ to $12.5c/\omega_i$ after they cross the shock wave. The ratio corresponds well to the inverse of the compression jump in the plasma density, $r \sim 2$. The thickness of CSs upstream is also compressed and becomes smaller than the ion inertial length, which is a favorable condition for the tearing instability [5]. Due to the instability, several magnetic reconnections occur and magnetic islands begin to appear after $x = 100c/\omega_i$ as one can see in the density plot of Fig. 2 and then these islands grow larger and larger through merging with each other. When the size of an island is comparable to the separation distance between CSs downstream, islands begin to interact with the next current sheet. This is noticible in B_z and the density plot of Fig.2 around $x = 150c/\omega_i$. This results in the electromagnetic fields consequently becoming turbulent.

Non-thermal ions begin to appear downstream of the shock wave. Two energy spectra for ions are plotted in Fig. 3, each corresponding to a different region. The blue curve corresponds to the region $50 \leq x/(c/\omega_i) \leq 100$ and overlaps both the upstream and downstream. CSs are not fully reconnected in this region. The energy spectrum for this region shows that some ions are accelerated up to energies of around $50m_iV_A^2/2$. This acceleration is due to the shock potential at which particles are reflected and their energy gain is from the motional electric field

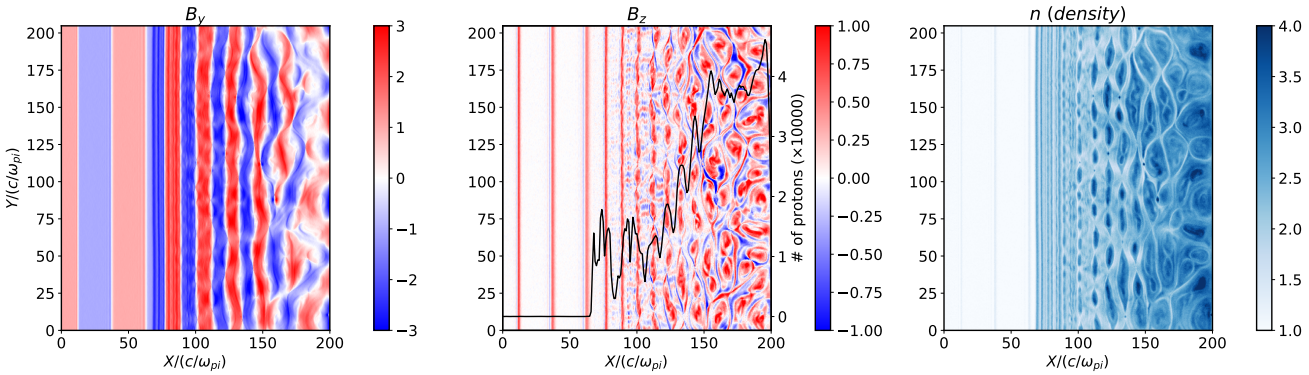

Figure 2. Snapshots of B_y, B_z, and the ion density from left to right at $T = 100\Omega_i^{-1}$, respectively. The black solid line in the middle panel is the ion flux calculated only for those particles with an energy above the threshold $v_i > 5V_A$, where v_i is the speed of an ion.

upstream. The red curve corresponds to the region $100 \leq x/(c/\omega_i) \leq 200$ and includes the far downstream region. The energy spectrum of this region shows a clear non-thermal distribution. The black dashed line is the Maxwell distribution function based on the downstream thermal temperature. Particles are accelerated up to almost $100 m_i V_A^2/2$. In this region, CSs are fully reconnected and electromagnetic fields are turbulent.

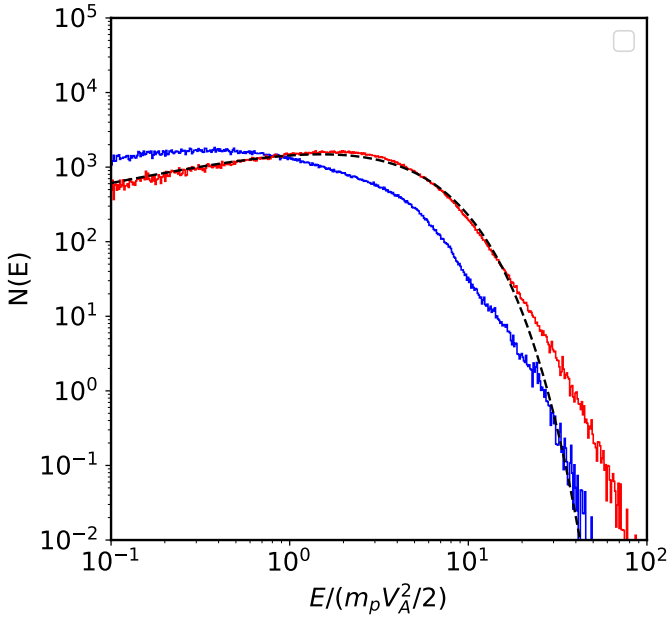

Figure 3. Energy spectra for ions at $T = 100\Omega_i^{-1}$. The blue and red lines are integrated in the ranges of $50 \leq x/(c/\omega_i) \leq 100$ and $100 \leq x/(c/\omega_i) \leq 200$, respectively. The black dashed line is a Maxwellian distribution with the downstream temperature.

The ion flux increases as magnetic reconnection develops downstream of the shock. We plot the integrated ion flux along the $y-$axis (the black line in the middle panel of Fig. 2) and choose only particles whose speed is larger than $5V_A$, i.e., we consider only non-thermal particles as shown in Fig. 3. The flux increase at the shock front indicates that some particles

are accelerated because of the shock wave. The flux stays constant after the shock wave until $50c/\omega_i$. We can interpret this distance as the point at which CSs start to experience reconnection and particle energization becomes significant. On the other hand, it is clear that the flux increases after $X = 125c/\omega_i$ and that there are some spikes which correspond to the location of CSs. Particles can be energized by several mechanism, such as island merging, contraction, and Fermi acceleration process, discussed in [12, 13, 14, 15]. A further analysis about the details of particle acceleration will be addressed in the near future. Finally, the energetic particle flux appears to saturate at $x = 150c/\omega_i$, but we need to perform longer and larger runs before we conclude that this is a physical effect.

4. Summary

We performed a 2D hybrid simulation to investigate the interaction of current sheets with a shock wave. In our simulation, the mean magnetic field of the multiple current sheets is in the plane of the simulation domain, unlike the simulation of [9]. This configuration allows magnetic reconnection to develop between current sheets in our simulation. We set the upstream thickness of a current sheet to be larger than the ion inertial length. The thickness and separation reduce to less than the ion inertial length and $\sim 12.5c/\omega_i$ after crossing the shock wave, respectively. Magnetic reconnection develops downstream due to the tearing instability and the electromagnetic fields become turbulent. In this simulation, we observed downstream flux enhancements. However, flux enhancements are not seen when multiple current sheets are absent (not shown here). We conclude that the energetic particle enhancements are due to magnetic reconnection downstream and our results support models that explain flux enhancements downstream of the heliospheric termination shock and an interplanetary shock wave [3, 4, 16]. In principle, when applying this system to the heliospheric termination shock, we must consider the modification due to pickup ions [17].

Acknowledgments

We acknowledge the partial support of the NSF/DOE Partnership in Basic Plasma Science and Engineering via NSF grant PHY-1707247 and by a NSF EPSCoR RII-Track-1 Cooperative Agreement OIA-1655280.

References

[1] Stone E, Cummings A, McDonald F, Heikkila B, Lal N and Webber W 2005 *Science* **309** 2017–2020
[2] Stone E C, Cummings A C, McDonald F B, Heikkila B C, Lal N and Webber W R 2008 *Nature* **454** 71–74
[3] Zhao L L, Zank G, Chen Y, Hu Q, le Roux J, Du S and Adhikari L 2019 *The Astrophysical Journal* **872** 4
[4] Zank G, Hunana P, Mostafavi P, Le Roux J, Li G, Webb G, Khabarova O, Cummings A, Stone E and Decker R 2015 *The Astrophysical Journal* **814** 137
[5] Drake J, Opher M, Swisdak M and Chamoun J 2010 *The Astrophysical Journal* **709** 963
[6] Burgess D, Gingell P and Matteini L 2016 *The Astrophysical Journal* **822** 38
[7] Burgess D and Schwartz S 1988 *Journal of Geophysical Research: Space Physics* **93** 11327–11340
[8] Tsubouchi K and Matsumoto H 2005 *Journal of Geophysical Research: Space Physics* **110**
[9] Giacalone J and Burgess D 2010 *Geophysical research letters* **37**
[10] Sironi L and Spitkovsky A 2011 *The Astrophysical Journal* **741** 39
[11] Winske D, Yin L, Omidi N, Karimabadi H and Quest K 2003 Hybrid simulation codes: Past, present and future—a tutorial *Space plasma simulation* (Springer) pp 136–165
[12] Drake J, Swisdak M, Che H and Shay M 2006 *Nature* **443** 553–556
[13] Oka M, Phan T D, Krucker S, Fujimoto M and Shinohara I 2010 *The Astrophysical Journal* **714** 915
[14] Zank G l, Le Roux J, Webb G, Dosch A and Khabarova O 2014 *The Astrophysical Journal* **797** 28
[15] Du S, Guo F, Zank G P, Li X and Stanier A 2018 *The Astrophysical Journal* **867** 16
[16] Adhikari L, Khabarova O, Zank G P and Zhao L L 2019 *The Astrophysical Journal* **873** 72
[17] Zank G P, Adhikari L, Zhao L L, Mostafavi P, Zirnstein E and McComas D J 2018 *The Astrophysical Journal* **869** 23